AGU PUBLICATIONS

Geochemistry, Geophysics, Geosystems

RESEARCH ARTICLE
10.1002/2014GC005453

Enhanced N_2-fixation and NH_4^+ recycling during oceanic anoxic event 2 in the proto-North Atlantic

I. Ruvalcaba Baroni[1], I. Tsandev[1], and C. P. Slomp[1]

[1]Faculty of Geosciences, Utrecht University, Utrecht, Netherlands

Key Points:
- Both N_2-fixation and upwelling of recycled NH_4^+ were enhanced during OAE2
- N_2-fixation was widespread while denitrification was important in the open ocean
- N_2-fixation was the major source of N in the proto-North Atlantic

Supporting Information:
- Readme
- Supplementary Information

Correspondence to:
I. Ruvalcaba Baroni,
i.ruvalcababaroni@uu.nl

Citation:
Ruvalcaba Baroni, I., I. Tsandev, and C. P. Slomp (2014), Enhanced N_2-fixation and NH_4^+ recycling during oceanic anoxic event 2 in the proto-North Atlantic, *Geochem. Geophys. Geosyst.*, *15*, 4064–4078, doi:10.1002/2014GC005453.

Received 9 JUN 2014
Accepted 3 OCT 2014
Accepted article online 8 OCT 2014
Published online 24 OCT 2014

Abstract Evidence from sediment core records and model studies suggests that increased nutrient supply played a key role in the initiation of the Cenomanian-Turonian oceanic anoxic event 2 (OAE2; 94 Ma). However, the relative roles of nitrogen (N) and phosphorus (P) availability in controlling primary productivity during the event are not fully understood. Here we expand an existing multibox model of the coupled cycles of P, carbon, and oxygen in the proto-North Atlantic by adding the marine N cycle. With the updated version of the model, we test the hypothesis that enhanced availability of P can fuel N_2-fixation, increase primary productivity and drive large parts of the proto-North Atlantic to anoxia during OAE2. In a sensitivity analysis, we demonstrate that N dynamics in the proto-North Atlantic respond strongly to variations in oxygen and P supply from the Pacific Ocean and to changes in circulation. The implemented N cycle weakly modifies the carbon cycle, implying that P was the major nutrient controlling primary productivity during OAE2. Our model suggests that both N_2-fixation and upwelling of recycled NH_4^+ were enhanced during OAE2 and that N_2-fixation was the major source of N in the proto-North Atlantic. Denitrification was more important in the water column than in sediments, with high rates in the open ocean and in the Western Interior. High P inputs in the proto-North Atlantic led to widespread N_2-fixation, which more than compensated for the loss of N through denitrification. As a consequence, rates of primary productivity and organic carbon burial were high.

1. Introduction

In the mid-Cretaceous greenhouse world, severe oxygen depletion occurred in oceanic bottom waters over extended periods of time. During these so-called oceanic anoxic events (OAEs), black shales formed on the seafloor. The deposition and burial of organic-rich sediments during the OAE of the Cenomanian-Turonian (OAE2; 94 Ma) have been attributed to high primary productivity and enhanced organic matter preservation [e.g., *Kuypers et al*., 2002; *Jenkyns*, 2010]. Sediment records for OAE2 [e.g., *Schlanger and Jenkyns*, 1976; *Mort et al*., 2007; *Jenkyns*, 2010; *Ruvalcaba Baroni et al*., 2014] and model studies [e.g., *Handoh and Lenton*, 2003; *Monteiro et al*., 2012] support a scenario where increased nutrient availability may have played a key role in maintaining the high productivity of OAE2. The long-term coupling between phosphorus (P) and nitrogen (N) dynamics and their role in controlling primary productivity [e.g., *Weber and Deutsch*, 2010] are, however, not fully understood. The same holds for the spatial trends in nutrient dynamics in the proto-North Atlantic during OAE2. Moreover, recent findings on the removal of fixed N under low-oxygen conditions (e.g., canonical denitrification and anammox) and on the conversion of atmospheric dinitrogen into organic matter by photoautotrophic organisms (i.e., N_2-fixation) are changing the general understanding of the N cycle [e.g., *Weber and Deutsch*, 2012; *Lam and Kuypers*, 2011].

The transition of a marine system from oxic to largely anoxic conditions leads to major changes in the sinks and sources of N. Denitrification (hereafter used to refer to all forms of inorganic N removal, thus including anammox) is constrained to redox interfaces in the water column [e.g., *Lam and Kuypers*, 2011; *DeVries et al*., 2013] or sediments [*Middelburg et al*., 1996; *Risgaard-Petersen et al*., 1993] where oxygen is below ~10 μmol L^{-1} and nitrate/nitrite concentrations are high. In the modern ocean, water-column denitrification, which has been estimated to account for about 35% of total global N losses [*DeVries et al*., 2013], is largely restricted to oxygen deficient zones in the open ocean and in coastal seas such as the Baltic Sea. Major loss of N through benthic denitrification is observed in productive coastal upwelling areas [*Lenton and Watson*, 2000; *Moore et al*., 2013] and on continental shelves [e.g., *Galloway et al*., 2004; *Codispoti*, 2007], where it may provide a negative feedback that tends to maintain nitrate as the limiting nutrient [*Lenton and Watson*,

2000; *Flögel et al*., 2011; *Moore et al*., 2013]. The onset of widespread anoxia is expected to lead to a decline in rates of sediment denitrification and a rise in pelagic denitrification.

Biological N_2-fixation is known to occur in regions where nitrate poor and phosphate-rich waters are upwelled [*Tyrrell*, 1999]. N_2-fixation fills the nitrate deficit and can potentially enhance marine productivity [*Falkowski*, 1997]. Benthic N_2-fixation is common in estuaries, coral reefs, salt marshes, and mangroves and contributes to the global N pool [*Capone and Carpenter*, 1982; *Bertics et al*., 2013].

Recent studies suggest a nearly balanced N cycle in the modern ocean [*DeVries et al*., 2013] with high rates of water-column and sediment denitrification [e.g., *Middelburg et al*., 1996; *Codispoti*, 2007]. This implies higher rates of N_2-fixation and a more widespread occurrence of this process [e.g., *Gruber*, 2004; *Gruber and Galloway*, 2008] than suggested by measurements for the modern ocean (supporting information Table S1). N_2-fixation has been shown to occur in nutrient-rich coastal upwelling systems and in suboxic intermediate waters, suggesting that the sources and sinks of N may be more closely and spatially connected than previously thought [*Fernandez et al*., 2011].

Our knowledge of N dynamics during OAE2 is limited and is mostly based on stable isotope analyses of sedimentary organic N (δ^{15}N). Low δ^{15}N of OAE2 sediments in the proto-North Atlantic has been interpreted to reflect high cyanobacterial N_2-fixation in N-depleted surface waters [*Kuypers et al*., 2004a; *Junium and Arthur*, 2007; *Ohkouchi et al*., 2006; *Blumenberg and Wiese*, 2012]. This is supported by the abundance of a qualitative biomarker for cyanobacteria in OAE2 sediments [*Kuypers et al*., 2004a]. Combined with elevated total organic carbon to total P ratios (TOC/P_{TOT}), this suggests that enhanced recycling of P from organic matter and high N_2-fixation provided the nutrients to sustain the high productivity during OAE2 [*Kuypers et al*., 2004a; *Junium and Arthur*, 2007]. However, there is a significant difference between the average δ^{15}N values in modern environments, where N_2-fixation is known to be important, and those during OAE2. This has been attributed to N_2 fixers using an alternative nitrogenase enzyme as a response to a molybdenum deficit in the water column [*Zhang et al*., 2014].

In anoxic waters, ammonium (NH_4^+) produced through decomposition of organic matter cannot be nitrified [*Omstedt et al*., 2009] and may accumulate in bottom waters. This recycled NH_4^+ will then be an important source of N for phytoplankton growth when upwelled to the surface. Based on δ^{15}N records of chlorophyll-derived porphyrins at Demerara Rise, *Higgins et al*. [2012] suggest that the difference between the modern isotopic signature for N_2 fixing environments and the more negative signature during OAE2 was not caused by cyanobacterial activity alone, but was mainly driven by direct NH_4^+ uptake from upwelling waters. They suggest that N_2-fixation may have contributed only $\sim$20% of the N supply for new production during OAE2. However, N_2-fixation likely varied spatially during OAE2 and therefore, its relative contribution compared to upwelling of recycled NH_4^+ in the entire proto-North Atlantic remains unclear.

While various recent global model studies of ocean biogeochemistry during OAE2 include the N cycle, N dynamics were not presented in the corresponding papers [*Flögel et al*., 2011; *Monteiro et al*., 2012]. Here we expand a multibox model, which describes the cycles of water, carbon, oxygen, and P in the proto-North Atlantic with the N cycle. With the new model, we test whether enhanced availability of P can fuel N_2-fixation, increase primary productivity, and drive large parts of the proto-North Atlantic to anoxia during OAE2. We assess the role of NH_4^+ in upwelled anoxic waters and its influence on primary productivity. We also determine whether or not there is a spatial coupling between denitrification and N_2-fixation. Finally, we study the response of N dynamics in the proto-North Atlantic to changes in ocean circulation and changes in oxygen and P supply from bottom waters of the Pacific Ocean. Our model is unique in that it distinguishes between processes in the coastal and open ocean in the proto-North Atlantic.

2. Model Description

A detailed multibox model of the proto-North Atlantic [*Ruvalcaba Baroni et al*., 2014] is expanded by adding the N cycle. The water cycle is extracted from the results of a regional water circulation model [*Topper et al*., 2011], which is specifically adapted to the paleobathymetry and atmospheric conditions of the proto-North Atlantic in the mid-Cretaceous. Note that the proto-North Atlantic represents about 5% of the surface area of the global ocean in the mid-Cretaceous.

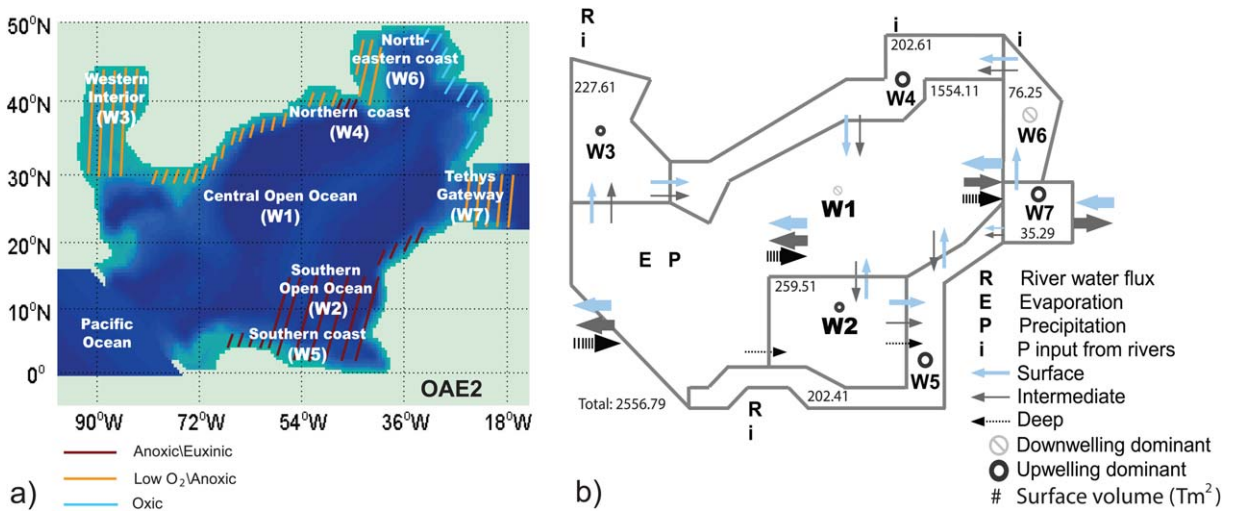

Figure 1. (a) Map of the proto-North Atlantic showing the bathymetry for OAE2, where the dark blue color indicates a water depth of >700 m and light blue a depth of <700 m. Superimposed, the shaded areas represent an approximation of the oxygen conditions in bottom waters as deduced from records of several redox proxies [e.g., *Sinninghe Damsté and Köster*, 1998; *Kuypers et al*., 2002; *Nederbragt et al*., 2004; *Kraal et al*., 2010b] and model studies [e.g., *Monteiro et al*., 2012; *Ruvalcaba Baroni et al*., 2014]. Corresponding areas in the model boxes are indicated. (b) Schematic showing the subdivision of the proto-North Atlantic into seven boxes (not to scale) for OAE2 conditions as implemented in our model. The model takes into account the increased water cycle and increased size of continental shelves due to sea level rise. The symbols R, E, and P indicate locations where river water fluxes, evaporation, and precipitation are included in the model. Horizontal arrows indicate lateral flows of water. The regions dominated by upwelling and downwelling are also indicated. Enlarged symbols indicate a significant increase in the water flux during OAE2. The numbers correspond to the volume of surface waters for each box. The total volume of surface waters is indicated.

During OAE2, both vertical and lateral transports of water on the shelves and in the surface and deep ocean in the proto-North Atlantic may have increased relative to pre-OAE2 conditions. This suggested increase in ocean circulation was mainly due to sea level rise and resulting changes in paleogeography [*Trabucho Alexandre et al*., 2010; *Topper et al*., 2011]. Therefore, we consider two settings for the water cycle, one for pre-OAE2 and other for OAE2 conditions, as explained in *Ruvalcaba Baroni et al*. [2014]. For both settings, the proto-North Atlantic is divided into seven boxes (Figure 1). The model segmentation is based on the areas of upwelling and downwelling as described in *Topper et al*. [2011]. Two open ocean boxes (the central, W1, and the southern open ocean, W2) are defined and divided vertically into a surface (0–100 m), intermediate (100–700 m), and deep bottom water (700–5000 m) box. Five additional boxes are located in coastal areas which include part of the continental slope (the Western Interior, W3, the northern, W4, the southern, W5, the north-eastern coast, W6, and the Tethys Gateway, W7). These coastal boxes are divided vertically into surface water (0–100 m) and shallow bottom water (100–700 m).

The original biogeochemistry of the multibox model is described in *Ruvalcaba Baroni et al*. [2014]. Here we only present new implementations, which are all linked to the N cycle. We account for three forms of N: nitrate and nitrite (NO_x^-), NH_4^+, and particulate organic N (PON). We assume only NO_x^- in surface waters, as oxygen concentrations in surface waters are always equilibrated with the atmosphere and thus, all NH_4^+ is expected to be nitrified to NO_x^-. The processes included for the N cycle are: formation of PON (NO_x^- uptake for phytoplankton growth); degradation of PON (remineralization/ammonification); conversion of NH_4^+ to nitrate (nitrification); PON export from surface to subsurface waters; burial of PON; transport of NO_x^- and NH_4^+; denitrification in both sediments and the water column; and N_2-fixation in surface and subsurface waters, which include sediments.

2.1. Initial Conditions for the N Cycle

The initial N fluxes and reservoirs in the proto-North Atlantic are defined for pre-OAE2 conditions following the approach used in other studies [e.g., *Flögel et al*., 2011; *Monteiro et al*., 2012]. The OAE2 water cycle is run with the initial biogeochemical conditions for pre-OAE2 in order to obtain the initial biogeochemical conditions for OAE2. The NO_x^- concentrations in each box are calculated by multiplying the soluble reactive P (SRP) concentrations by the mean modern N to P (N:P) ratio of water masses at similar depths. The processes related to PON (supporting information Figure S1.1) are linked to the carbon cycle [*Ruvalcaba Baroni et al*., 2014] via the Redfield ratio (C:N = 106:16) [e.g., *Rabouille et al*., 2001; *Wallmann*, 2003; *Slomp and Van Cappellen*, 2007].

Paleoceanographic proxies do not provide a quantitative measure of denitrification and N_2-fixation in the proto-North Atlantic before and during OAE2. We therefore use modern values to constrain these N fluxes. Denitrification for each box is estimated using values from the literature, taking into account the box size and oxygen concentrations given by the model. N_2-fixation rates are obtained by assuming a balanced initial N cycle. The N cycle, as implemented in the model, is summarized in supporting information Figure S1.1. Reservoir sizes and N fluxes for each box are listed in supporting information Tables S1.1, S1.2, and S1.3.

Global rates of denitrification (including anammox) have been estimated to be as high as 28 Tmol yr^{-1} [*Codispoti*, 2007]. However, reported rates in the literature show a broad range (supporting information Table S1). Here we assume a value of 28 Tmol yr^{-1} for both water-column and sediment denitrification in the modern ocean. We assume low rates in oxic bottom waters and higher rates where transient anoxia occurred. This is in line with the lateral distribution of denitrification in the modern ocean [*Middelburg and Levin*, 2009; *DeVries et al.*, 2013].

In our model, we include sedimentary and subsurface N_2-fixation, besides N_2-fixation in surface waters. Our estimation of total N_2-fixation in the proto-North Atlantic is relatively high (~20% of the highest modern global estimate of N_2-fixation; supporting information Table S1). This is reasonable given that N_2-fixation may rise with increasing temperature and atmospheric CO_2 [*Hutchins et al.*, 2007], in line with the greenhouse conditions during the Cretaceous.

2.2. Rate Laws for N Fluxes

Many types of microbial activity are involved in the different pathways of the N cycle, several of which depend on the dissolved oxygen present in the water. The relationship between nutrient concentrations and biological N fluxes is generally highly nonlinear. In this section, a detailed description of the parameterization of each modeled N process is presented. A summary of the major equations for all cycles in oxic conditions and the nonlinear equations for the N cycle is given in supporting information Tables S1.4.1 and S1.4.2, respectively.

2.2.1. Organic Nitrogen Processes

Primary productivity (*PP*) is assumed to be colimited by P and N, following Liebig's law:

$$PP = kphoto \cdot Red_{C:P} \cdot W \cdot min\left(\frac{[NO_x^-]}{16} \cdot \frac{[NO_x^-]}{[NO_x^-]+K_N}, [SRP] \cdot \frac{[SRP]}{[SRP]+K_P}\right), \quad (1)$$

where *kphoto* is the rate constant for primary productivity, $Red_{C:P}$ is the Redfield C:P ratio (106:1), and W is the water reservoir where the process is occurring. The brackets represent the concentrations and K_N and K_P are the half saturation concentrations for phytoplankton growth for N and P as a limiting nutrient, respectively (supporting information Table S1.4.3).

While remineralization of PON in surface waters is assumed to transform PON directly to NO_x^-, degradation of PON below the surface waters leads to NH_4^+ production. In intermediate waters, remineralization of POC ($POCREM_i$) and, therefore, degradation of PON ($AMMONI_i$) are reduced with low-oxygen concentrations ($O_2^{low} < 5\ \mu$mol L^{-1}) [*Andersson et al.*, 2008; *Middelburg and Levin*, 2009]:

$$AMMONI_i = POCREM_i(O_2^{low}) \cdot Red_{N:C}, \quad (2)$$

where $Red_{N:C}$ is the N:C Redfield ratio (16:106). Burial of PON follows the original parameterization of burial of organic carbon [*Ruvalcaba Baroni et al.*, 2014] multiplied by $Red_{N:C}$.

2.2.2. N_2-Fixation

N_2-fixation in surface waters is limited by the availability of P [e.g., *Sañudo-Wilhelmy et al.*, 2001; *Dyhrman et al.*, 2007; *Knapp et al.*, 2012], iron (Fe) [e.g., *Karl et al.*, 2002; *Mills et al.*, 2004], and several trace metals [*Howarth et al.*, 1988; *Falkowski*, 1997; *Zerkle et al.*, 2006] and is inhibited by high dissolved nitrate [*Wallmann*, 2003; *Knapp et al.*, 2012]. Other processes affecting N_2-fixation include light intensity [*Carr and Whitton*, 1982; *Falcón et al.*, 2004], temperature [*Staal et al.*, 2003; *Breitbarth et al.*, 2007], and atmospheric CO_2 [*Hutchins et al.*, 2007]. N_2 fixing organisms living in surface waters differ from those living below or in

sediments. The latter may be additionally limited by a low influx of organic matter to the sea floor [*Fulweiler et al.*, 2008] and high NH_4^+ concentrations [*Howarth et al.*, 1988].

Here we assume that N_2-fixation in both surface and subsurface waters ($NFIX_s$ and $NFIX_{sub}$) are dependent on SRP and are inhibited by NO_x^- (equations (3) and (4)). We assume that Fe does not limit N_2-fixation during OAE2, due to high inputs of Fe from hydrothermal vents associated with submarine volcanism [*Vermeij*, 1995] and from biological Fe reduction in low-oxygen environments [e.g., *Moffett et al.*, 2007]. N_2-fixation is assumed to directly add inorganic N to the NO_x^- pool. The subsurface N_2-fixation includes sedimentary N_2-fixation and is also inhibited by high NH_4^+ concentrations (equation (4)). N_2-fixation is defined as follows:

$$NFIX_s = knf_s \cdot W \cdot 16 \cdot [SRP] \cdot \frac{[SRP]}{[SRP]_o} \cdot \left(\frac{K_{NF}}{[NO_x^-] + K_{NF}} \right)^{nfNs}, \tag{3}$$

$$NFIX_{sub} = knf_{sub} \cdot W \cdot 16 \cdot \left([SRP] \cdot \frac{[SRP]}{[SRP]_o} \right)^{nfP} \cdot \left(\frac{K_{NF}}{[NO_x^-] + [NH_4^+] + K_{NF}} \right)^{nfNb}, \tag{4}$$

where knf_s and knf_{sub} are the rate constants of N_2-fixation in surface and subsurface waters, respectively. The factor $\frac{[SRP]}{[SRP]_o}$ allows a high sensitivity to SRP with a small initial SRP concentration ($[SRP]_o = 0.01$ μmol L^{-1}). The limitation of NO_x^- is calculated assuming Monod kinetics [*Wallmann*, 2003]. In the surface waters, however, this limitation is reduced when the surface N:P ratios are low via the factor $nfNs = 2 - \frac{16}{N:P}$. The sensitivity of surface N_2-fixation to both SRP concentrations and N:P ratios (which determine the value of *nfNs*) is shown in supporting information Figure S1.5.1. N_2-fixation is considered to be impacted less by NO_x^- in subsurface than in surface waters and, therefore, we assume a constant factor *nfNb* of 0.5. K_{NF} is the Monod constant for N_2-fixation at low latitudes (supporting information Table S1.4.3). To account for the possible limiting factors for subsurface N_2-fixation, we assume that $NFIX_{sub}$ is nonlinearly related to SRP. This is represented by including the term *nfP* (equation (4)). Its small value (0.01) makes subsurface N_2-fixation less dependent on SRP than that in surface waters (supporting information Figure S1.5.2a).

2.2.3. Nitrification

Nitrification is a key process controlling NH_4^+ concentrations in the water column. Its rate depends on both the oxygen and NH_4^+ concentrations [*Kantartzi et al.*, 2006]. Here we define nitrification (*NITRI*) as being linearly dependent on NH_4^+ and nonlinearly dependent on oxygen by assuming Monod kinetics. When oxygen concentrations below surface waters are above 30 μmol L^{-1}, the parameterization of *NITRI* is as follows:

$$NITRI = knox \cdot [NH_4] \cdot W \cdot \frac{[O_2]}{[O_2] + K_{O2}}. \tag{5}$$

In low-oxygen conditions, nitrification decreases significantly. In anoxic waters, it comes to a halt. With decreasing nitrification, NH_4^+ starts to build up in the water column [e.g., *Konovalov et al.*, 2008; *Lam et al.*, 2009]. To capture these dynamics, we assume that the dependency of nitrification on NH_4^+ is negligible when oxygen concentrations are below 30 μmol L^{-1} and equation (5) becomes:

$$NITRI = knlox \cdot [NH_4] \cdot W \cdot \frac{[O_2]}{[O_2] + K_{O2}} \cdot \frac{K_{NH4}}{[NH_4] + K_{NH4}}. \tag{6}$$

In equations (5) and (6), *knox* and *knlox* are the rate constants for nitrification in oxic and low-oxygen waters, respectively. K_{O2} and K_{NH4} are the Monod constants for oxygen and NH_4^+ (supporting information Table S1.4.3).

2.2.4. Denitrification

Denitrification has been measured in modern marine environments where oxygen concentrations are lower than 10 μmol L^{-1} and NO_x^- concentrations are high (e.g., Black sea, Arabian Sea). Denitrification typically increases with decreasing oxygen concentrations; maximum values occur in waters with oxygen concentrations of $\sim$2 μmol L^{-1} [e.g., *Codispoti et al.*, 2005; *Murray et al.*, 1995]. Denitrification is also nonlinearly dependent on NO_x^- [*Middelburg et al.*, 1996]. In the model, we use a square root relationship [*Middelburg et al.*, 1996] to describe this nonlinear dependency relative to NO_x^- for both the water column (*DENW*) and

sediments (*DENS*). In our parameterization of denitrification, the oxygen dependency and NO_x^- limitation are assumed to follow Monod kinetics:

$$DENW = \sqrt{kdenw \cdot [NO_x^-] \cdot W} \cdot \frac{[NO_x^-]}{[NO_x^-]+K_{NO}} \cdot \left(\frac{K_{O2}}{[O_2]+K_{O2}}\right)^{dnfO}, \quad (7)$$

$$DENS = \sqrt{kdens \cdot [NO_x^-] \cdot W} \cdot \frac{[NO_x^-]}{[NO_x^-]+K_{NO}} \cdot \frac{K_{O2}}{[O_2]+K_{O2}}, \quad (8)$$

where *kdenw* and *kdens* are the rate constants for denitrification in the water column and sediments, respectively. K_{NO} is the Monod constant for NO_x^- involved in denitrification (supporting information Table S1.4.3).

Water column denitrification occurs in well-demarcated areas within low-oxygen zones [*Naqvi et al*., 2006], a feature that is not fully captured in our box model. Therefore, denitrification in the water column is activated before the entire box reaches an oxygen concentration of 10 μmol L^{-1}. Since our parameterization of denitrification is a continuous function relative to oxygen, we add an exponential factor to the Monod kinetics in the water column (*dnfO*). This number is obtained through a sensitivity analysis (1.8 for intermediate and coastal bottom waters and 1.5 for open bottom waters; supporting information Figure S1.5.2b, S1.5.2c, and S1.5.2d). Consequently, denitrification in the water column significantly increases when oxygen concentrations fall below 30 μmol L^{-1}. When bottom waters are anoxic, water-column denitrification is no longer dependent on oxygen (i.e., $\frac{K_{O2}}{[O_2]+K_{O2}} = 1$ in equation (7)). Sediments are generally more reducing than the overlying water column and therefore, in our parameterization, denitrification in sediments is more widespread.

2.3. Numerical Experiments

Our specific interest is to understand whether N_2-fixation could have compensated for N-losses due to denitrification during OAE2. We study under which conditions N_2-fixation can sustain high primary productivity and we analyze the relationship between sources and sinks of N in oxygen depleted waters. The rates and spatial trends of the major N processes in the proto-North Atlantic are simulated, including the contribution of upwelling of recycled NH_4^+ to phytoplankton growth in surface waters. We also assess which element, N or P, likely limited primary productivity in the proto-North Atlantic.

We start from the final scenario of the original model describing the dynamics of oxygen, carbon and P during OAE2 (experiment E7 in *Ruvalcaba Baroni et al*. [2014]). This baseline run assumes a threefold increase in weathering from pre-OAE2 to OAE2 [*Blättler et al*., 2011], low-oxygen concentrations in Pacific bottom waters, and a reduced ocean circulation (detailed assumptions in Table 1). Sediment records of trace metals [e.g., *Kuypers et al*., 2004b; *Owens et al*., 2012] and TOC/P_{TOT} ratios (N. A. G. M. van Helmond et al., Spatial extent and degree of oxygen depletion in the deep proto-North Atlantic basin during Oceanic Anoxic Event 2, 2014) for the deep proto-North Atlantic suggest anoxic bottom waters. A decrease in overturning with respect to the original ocean circulation as calculated by *Topper et al*. [2011] is required in our model for the bottom waters of the central open ocean (W1b) to be close to anoxia (~5 μmol L^{-1}). The base line run with the original model is termed BsLi-P, whereas the same run with the model expanded with the N cycle is termed BsLi-N. The concentrations of NH_4^+ and NO_x^- in the bottom waters of the Pacific Ocean in the BsLi-N run are assumed to be 15 and 0 μmol L^{-1}, respectively, which are typical values for modern low-oxygen waters, such as observed in the Black and Arabian Sea [e.g., *Konovalov et al*., 2000; *Naqvi et al*., 2006].

We perform three numerical experiments (Table 1) to assess the model response to changes in SRP (Experiment 1), oxygen concentrations in Pacific bottom waters (Experiment 2) and in ocean circulation (Experiment 3). For experiment 2, we linearly increase the NH_4^+ concentrations and decrease NO_x^- when oxygen concentrations decrease below 30 μmol L^{-1} in Pacific bottom waters. As the SRP concentrations in the ocean likely remained relatively constant over the Phanerozoic [*Planavsky et al*., 2010], we set the maximum increase of SRP from the Pacific Ocean in experiment 1 to 1.3 times the mean concentrations for modern Pacific bottom waters (~3 μmol L^{-1}). The experiments are compared to the results obtained with the original model [*Ruvalcaba Baroni et al*., 2014].

The model is run to steady state, which takes approximately 10 kyrs. The N cycle reaches steady state after 500 years. We first analyze the results of the three sensitivity experiments and compare them to the results of the original model. We then describe the results of the BsLi-N run and discuss the general biogeochemical implications for the proto-North Atlantic.

Table 1. Summary of Experiments Starting From the BsLi-P [*Ruvalcaba Baroni et al.*, 2014] and BsLi-N Runs for OAE2 Conditions[a]

Experiments	Description	No. of Runs
BsLi-P	Weathering P supply of 0.03 Tmol yr^{-1} (three times pre-OAE2 value), erosive P input of 0.001 Tmol yr^{-1}, SRP and oxygen concentrations in Pacific bottom waters of 2.9 and 5 μmol L^{-1}, respectively and 70% of the original ocean circulation[b]	1
BsLi-N	Same as BsLi-P plus NH_4^+ and NO_x^- concentrations in Pacific bottom waters of 15 and 0 μmol L^{-1}, respectively	1
Experiment 1	Changes in SRP concentrations from Pacific bottom waters (from 1.3 to 3.8 μmol P L^{-1}, which correspond to a flux of 0.6–1.8 Tmol P yr^{-1})	9
Experiment 2	Changes in oxygen concentrations from Pacific bottom waters (from 200 to 0 μmol O_2 L^{-1}) Changes in NO_x^- concentrations from Pacific bottom waters when $[O_2] < 30$ μmol L^{-1} (from 20 to 0 μmol NO_3^- L^{-1}) Changes in NH_4^+ concentrations from Pacific bottom waters when $[O_2] < 30$ μmol L^{-1} (from 0 to 25 μmol NH_4^+ L^{-1})	13
Experiment 3	Changes in ocean circulation (from 100% to 30% of the original overturning[b])	8

[a]The table details the total number of runs for each experiment (total number of runs adds up to 32).
[b]Original overturning (meridional = 15 Sv) from *Topper et al.* [2011].

3. Sensitivity Analysis

3.1. Oxygen Distribution

The spatial distribution of oxygen in the proto-North Atlantic is highly sensitive to changes in SRP and oxygen concentrations entering from the Pacific Ocean (Experiments 1 and 2, Figures 2a and 2b) and to ocean circulation (Experiment 3; Figure 2c). In all three experiments, significant regional differences in bottom-water oxygen can be observed. Bottom water anoxia in the central open ocean (W1b) is only achieved when conditions are close to those of the BsLi-N run. Further enhancing the input of SRP and decreasing the input of oxygen from Pacific bottom waters can amplify deep sea anoxia (Experiments 1 and 2, Figures 2a and 2b). To better constrain these last two parameters, more information about oxygen conditions and P dynamics in the deep Pacific would be needed.

Because N:P ratios in surface waters are always below Redfield in all three experiments (supporting information Figure S2.1a), primary productivity in the new version of the model is slightly lower than that of the original model. Consequently, oxygen concentrations in the new version of the model are somewhat higher than in the original model (Figures 2d, 2e, and 2f), notably along the northern and north-eastern coast (W4 and W6) and the Tethys Gateway (W7). These differences in oxygen (ΔO_2) are generally lower than $\sim$15 μmol L^{-1}, except in the southern open ocean (W2b) when the Pacific Ocean is well oxygenated. Thus, all experiments performed with the BsLi-P and BsLi-N runs yield similar oxygen concentrations. This suggests that P and not N is the main driver for anoxia during OAE2. Our results are consistent with those of other authors [e.g., *Tsandev and Slomp*, 2009; *Monteiro et al.*, 2012], and further validate the concept that P acted as a major driver for anoxia in the proto-North Atlantic during OAE2. The positive ΔO_2 indicates that the addition of the N cycle in our model only moderates the impact of increased P loads on organic matter production and oxygen consumption.

Ocean circulation plays an important role in distributing oxygen and, thus, nutrients in the proto-North Atlantic. The sensitivity of dissolved oxygen to changes in ocean circulation (Experiment 3, Figure 2c) differs regionally. While reduced ocean circulation leads to a decrease in oxygen in bottom waters of both the open and coastal ocean, the response in the open ocean (W1 and W2) is less pronounced than along the coast. When low-oxygen conditions in the open bottom waters (W1b and W2b) are well established, deep bottom waters cannot simply reoxygenate by increasing ocean circulation. Oxygen concentrations below $\sim$5 μmol L^{-1} in bottom waters of the central open ocean (W1b) develop only when circulation is reduced to at least 70%. This ocean circulation intensity corresponds to a meridional ocean overturning of roughly 11 Sv (Sverdrup = 10^6 m^3 s^{-1}), which falls into the overturning range proposed by *Monteiro et al.* [2012] for the global Cretaceous ocean. This is also in line with molybdenum to total organic carbon ratios for three sites located in the central open ocean for the OAE2 interval that suggest a severely restricted but not stagnant ocean circulation (N. A. G. M. van Helmond et al., Spatial extent and degree of oxygen depletion in the deep proto-North Atlantic basin during Oceanic Anoxic Event 2, submitted to *Geochemistry, Geophysics, and Geosystems*, 2014). Note that the Pacific inflow and upwelling/downwelling in the proto-North Atlantic could be decoupled [*Topper et al.*, 2011]. However, any scenario with weak inflow from the Pacific Ocean would not allow anoxia to develop in the proto-North Atlantic (for further details we refer to *Ruvalcaba Baroni et al.* [2014]).

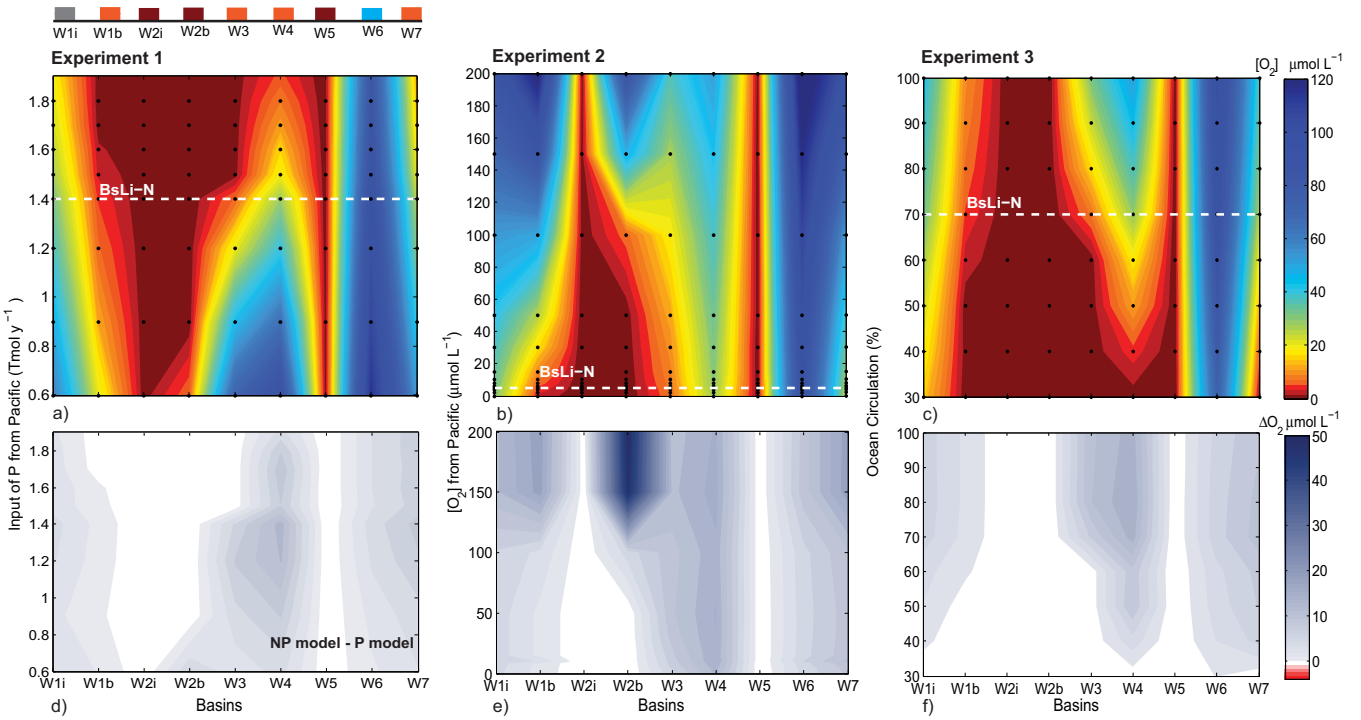

Figure 2. Oxygen distribution for (a) Experiment 1 (varied P input from the Pacific Ocean), (b) Experiment 2 (varied oxygen from the Pacific Ocean), and (c) Experiment 3 (varied ocean circulation). The BsLi-N run is indicated as a horizontal-dashed white line. The color bars above the *x* axis of Experiment 1 indicate the oxygen conditions for each basin as deduced from observations of several redox proxies for OAE2 (e.g., see compilation in *Ruvalcaba Baroni et al.* [2014]) where dark red denotes euxinic/anoxic; orange, low-oxygen/anoxic; blue, low-oxygen/oxic; and dark gray, uncertain. The indices i and b refer to intermediate and bottom waters. The bottom plot shows differences in oxygen concentration between the new and original model (ΔO_2= NP model − P model) for (d) Experiment 1, (e) Experiment 2, and (f) Experiment 3. Note that ΔO_2 is always positive.

3.2. N Dynamics

The dynamics of N in the proto-North Atlantic are strongly affected by the regional differences in biogeochemistry and redox conditions. This is reflected by the surface N:P ratios which, despite the efficient nutrient transport in the basin, show a spatial variability (supporting information Figure S2.1a). This regional trend is consistent across all three experiments. Bottom water N:P ratios are directly affected by local rates of denitrification and P recycling. This implies that biogeochemical processes counteract with the otherwise homogenous distribution of nutrients through physical transport (supporting information Figure S2.1b).

In Experiment 1, both regional (expressed in Tmol m^{-3} yr^{-1}) and total N_2-fixation (expressed in Tmol yr^{-1}) increase with increasing SRP from Pacific bottom waters (Figures 3a and 3b). While P input is the main driver for N_2-fixation, the relationship between N_2-fixation and SRP concentrations is nonlinear. For example, N_2-fixation decreases with respect to the maximum (at 1.4 Tmol P yr^{-1}) for a 1.5 Tmol P input per year^{-1} from the Pacific Ocean. This is due to high accumulation of NH_4^+ (not shown) under more widespread anoxia when P inputs increase (Figure 2a). Therefore, regional differences in redox conditions and N:P ratios together affect the response of N_2-fixation to P inputs. This is especially important in upwelling areas, where surface N_2-fixation is highest and, thus, a high primary productivity is maintained. The most pronounced changes in surface N_2-fixation (mol m^{-3} yr^{-1}), when the supply of SRP from the Pacific Ocean is increased, are observed for the Western interior (W3s) and the Tethys Gateway (W7s). For all three experiments, the regional response of N_2-fixation is similar to that shown in Figure 3a.

In Experiment 2, total N_2-fixation in the proto-North Atlantic responds nonlinearly to increasing oxygen from the Pacific Ocean (Figure 3c). When most of the proto-North Atlantic is low in oxygen, the accumulation of NH_4^+ inhibits N_2-fixation. As a consequence, total N_2-fixation is relatively low under fully anoxic conditions. With increasing oxygen, N_2-fixation increases at first, but subsequently decreases as denitrification is reduced, increasing the N pool and therefore, inhibiting N_2-fixation.

In Experiment 3 (Figure 3d), the most pronounced decrease in N_2-fixation (Tmol yr^{-1}) is observed when ocean circulation changes from 70% to 60%. Above 70%, N_2-fixation is mainly fueled by upward transport

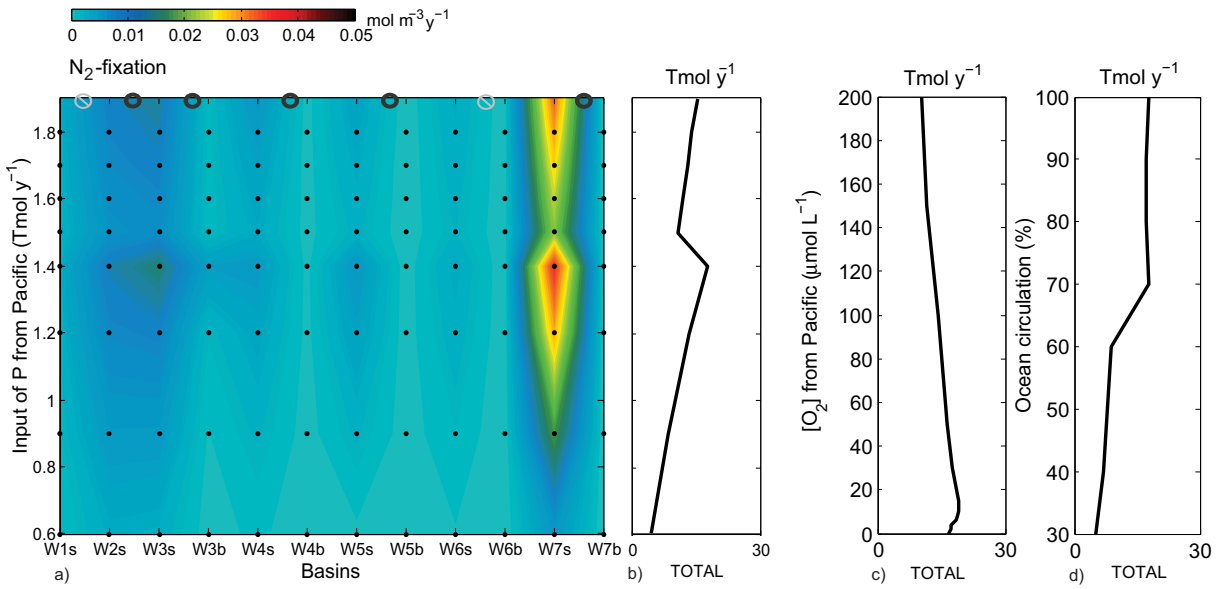

Figure 3. N_2-fixation in the proto-North Atlantic for Experiments 1, 2, and 3: (a) regional (contour plot); (b) total N_2-fixation for Experiment 1; (c) total N_2-fixation in the proto-North Atlantic for Experiment 2; (d) total N_2-fixation for Experiment 3. In Figure 3a, the regions dominated by upwelling (dark circles) or downwelling (gray circles) are indicated at the top of the figure. The index s refers to the surface waters, and other indices are as indicated in Figure 2.

of SRP. When ocean circulation decreases from 70% to 60%, both increased NH_4^+ and decreased SRP input from upwelling contribute to substantial decrease in N_2-fixation. With 70% circulation, denitrification is highest, because both sediment and water-column denitrification are highly active in most coastal regions. Across all three experiments, we see a high variation in total N_2-fixation rates (about 10 Tmol N yr^{-1}, Figures 3b–3d).

In our model, the proto-North Atlantic sits close to the threshold between P and N limitation due to high rates of N_2-fixation. If N_2-fixation rates were lower than assumed in our model, and if they did not respond to P inputs, primary productivity and organic matter burial required for an OAE2 would not have been sustainable. However, primary producers may have adapted their nutrient stoichiometry [e.g., *Flögel et al.*, 2011], a process not considered in this model. Based on our results, we conclude that SRP input from the Pacific Ocean, in addition to riverine P supply [e.g., *Flögel et al.*, 2011; *Ozaki et al.*, 2011; *Monteiro et al.*, 2012; *Ruvalcaba Baroni et al.*, 2014], was likely a major forcing for the biogeochemistry in the proto-North Atlantic during OAE2.

4. Implications for the Proto-North Atlantic

4.1. Scenario for OAE2

As demonstrated from Experiments 1–3, the LsBi-N run represents an optimal scenario, reproducing oxygen concentrations for OAE2. During the anoxic event, NH_4^+ accumulates in intermediate and bottom waters in most regions of the proto-North Atlantic because nitrification is limited by oxygen (Figure 4a). Spatial differences in NH_4^+ concentrations for OAE2 are largely related to variations in organic matter export rather than oxygen. The resulting NH_4^+ concentrations are within the range of those found in modern poorly oxygenated regions (20–40 μmol L^{-1}), such as in the Black Sea and Arabian Sea [e.g., *Konovalov et al.*, 2000; *Naqvi et al.*, 2006].

While NH_4^+ concentrations increase, NO_x^- concentrations decrease during OAE2 with respect to pre-OAE2 concentrations in all poorly oxygenated regions of the proto-North Atlantic. This denotes an important shift of the available inorganic N in the proto-North Atlantic from NO_x^- to NH_4^+, which is in line with recycling of N in bottom waters.

In pre-OAE2 conditions, all regional N:P ratios in the model are close to Redfield. During OAE2, the ratios in surface waters are spatially variable and are mostly below Redfield (Figure 4b). This is in agreement with observations of modern N:P ratios in low-oxygen aquatic systems [e.g., *Wasmund et al.*, 2001; *Naqvi et al.*, 2006; *Quan and Falkowski*, 2009]. In the southern coastal box (W5) where euxinia can develop (Figures 4a

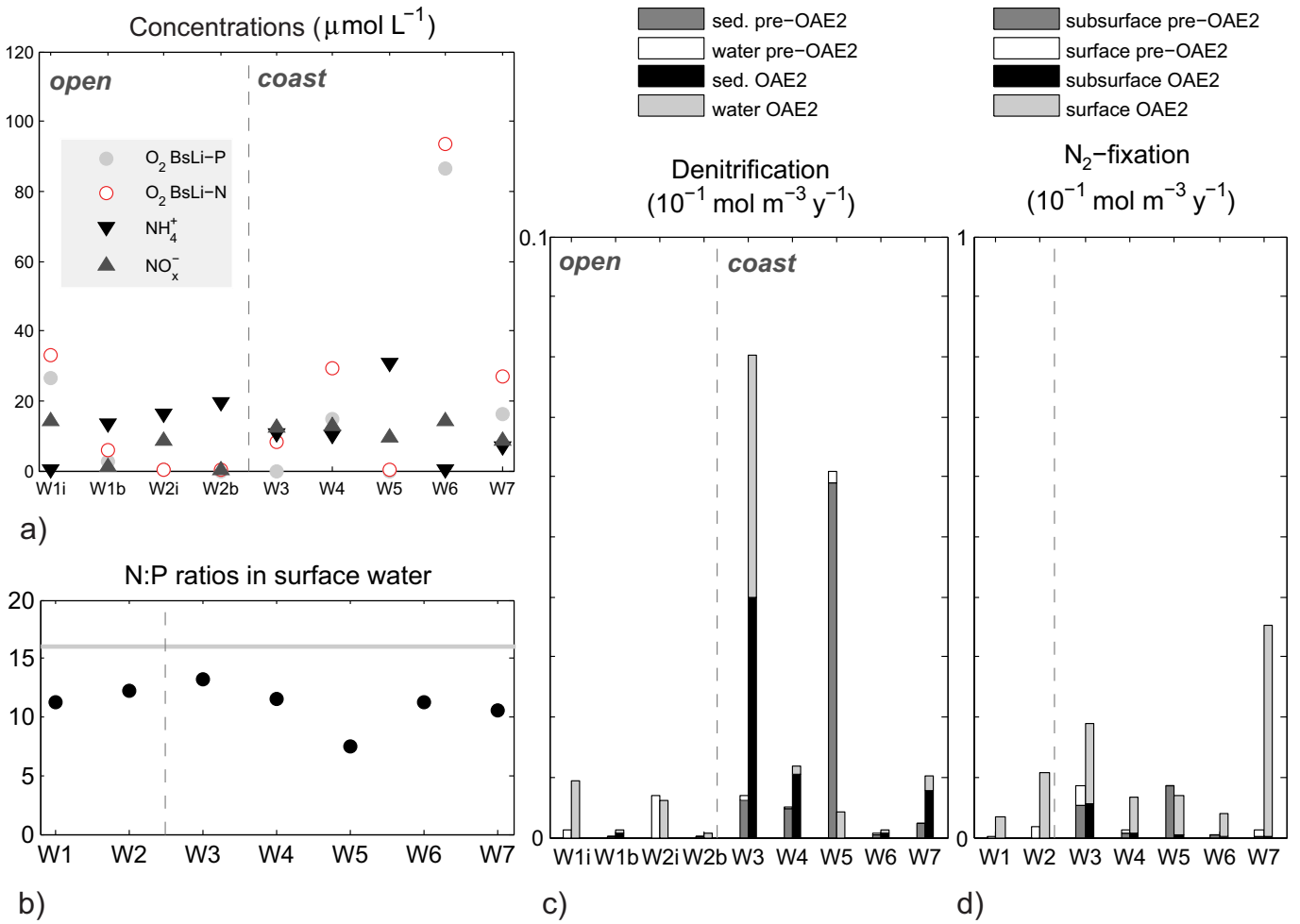

Figure 4. Key fluxes and concentrations for the N cycle in each basin of the proto-North Atlantic during OAE2 in the BsLi-N run: (a) oxygen (O_2), ammonium (NH_4^+), and nitrate (NO_x^-) concentrations, where the oxygen concentrations of the BsLi-P run are also plotted as a reference; (b) N:P ratios, where the horizontal gray line indicates the N:P Redfield ratio (16), as set for pre-OAE2 conditions; (c) sedimentary and water column in pre-OAE2 and OAE2 conditions; (d) surface and subsurface (including sedimentary) N_2-fixation for pre-OAE2 and OAE2. The vertical-dashed line separates the open from the coastal ocean. Indices are as indicated in Figure 2.

and 4b), the lowest surface N:P ratios are found despite the highest NH_4^+ concentrations in bottom waters. This is mainly due to enhanced P recycling under anoxic conditions. Note that the oxygen concentrations and therefore N:P ratios in this region could have been low before OAE2.

Due to the decrease in oxygen from pre-OAE2 to OAE2 conditions, denitrification increases in most regions of the proto-North Atlantic (Figure 4c). The highest rates per water volume are found along the coast (0.004, 0.001, 0.0004, and 0.001 mol m^{-3} yr^{-1} in W3, W4, W5, and W7, respectively). Coastal denitrification switches from mainly occurring in sediments before OAE2 to being more important in the water column during OAE2. In the southern coastal box (W5), however, water-column denitrification is significantly reduced due to low NO_x^- concentrations. This leads to a decrease in total N removal along the southern coast. In other coastal areas with low-oxygen (<30 μmol L^{-1}), water-column denitrification increases by a factor of ~2 (in W4 and W7) to about 40 (in W3) from pre-OAE2 to OAE2 conditions.

In the central open ocean (W1), denitrification rates per volume more than double from pre-OAE2 to OAE2, but remain low (~0.001 mol m^{-3} yr^{-1}) due to the lower NO_x^- concentrations relative to pre-OAE2 conditions. In the southern intermediate waters (W2i), water-column denitrification decreases due to NO_x^- limitation. In general, denitrification per water volume in the proto-North Atlantic increases by ~35% during OAE2 relative to pre-OAE2 conditions.

In contrast, N_2-fixation in the proto-North Atlantic more than triples during OAE2 (Figure 4d). N_2-fixation rates are generally one order of magnitude higher when expressed as mol m^{-3} yr^{-1} than denitrification rates, and are highest in the Tethys Gateway (W7). This suggests that N_2-fixation was a major process in the proto-North Atlantic during OAE2. The difference in magnitude between N_2-fixation and denitrification per water volume is due to the spatial decoupling of both processes. While N_2-fixation is mainly enhanced in surface waters during OAE2, denitrification occurs in bottom and intermediate waters. This indicates that moderate changes in total denitrification may coexist with large perturbations of N_2-fixation when P inputs are high. Thus, surface N:P ratios are mostly controlled by the amount of SRP reaching surface waters.

When comparing the results of the BsLi-P and the BsLi-N runs, rates of most processes involving carbon and P, such as primary productivity, burial of POC, and burial of total P are similar (supporting information Figure S2.2). The relative burial increase of POC in the BsLi-N run is in good agreement with the increase in POC content recorded in the sediments during OAE2 (supporting information Table S2). This implies at least a doubling in both regional and mean burial of POC in the proto-North Atlantic [e.g., *Sinninghe Damsté et al*., 2010; *Voigt*, 2000; *van Bentum et al*., 2012; *Owens et al*., 2012]. Such a doubling of POC burial can be achieved with a rate of primary productivity that is lower than the mean rate in modern upwelling zones ($\sim$150 mol C m^{-2} yr^{-1}) [*Millero*, 1996; *Fashman*, 2003]. Based on this result and the sensitivity analysis, we consider that the simulation of the BsLi-N run is a good approximation of the general biogeochemistry during the OAE2 interval.

4.2. Basin-Scale N Dynamics for OAE2

In the BsLi-N run, $\sim$78% of the proto-North Atlantic (with a total water volume of 62,527 Tm^3) is anoxic. During OAE2, this was equivalent to 4% of the global mid-Cretaceous ocean (with a total water volume of $\sim$1,348,600 Tm^3). At present, about 2% of the modern global ocean is anoxic [*Paulmier and Ruiz-Pino*, 2009].

In our simulation for OAE2, total primary productivity in the basin (1136 Tmol C yr^{-1}) is about 25% of the modern global rate ($\sim$4558 Tmol C yr^{-1}) [*Longhurst et al*., 1995; *Houghton*, 2007]. During OAE2, we find that total N_2-fixation (18 Tmol N yr^{-1}, Figure 5a) accounts for about 11% of the total N for new production (171 Tmol N yr^{-1}) in the proto-North Atlantic. This percentage is lower than the value of 20% estimated by *Higgins et al*. [2012]. However, their estimate is based on geological records of only one site in the southern proto-North Atlantic and may not be representative for the entire basin.

Total denitrification simulated by the BsLi-N run in the proto-North Atlantic (Figure 5a) is of a similar order of magnitude to total N_2-fixation. Therefore, while volumetric N_2-fixation is very intense in surface waters of the proto-North Atlantic, the total rate of N_2-fixation is comparable to total denitrification. Sedimentary denitrification in the proto-North Atlantic (4 Tmol yr^{-1}) accounts for only about 22% of total denitrification in our model. This is in agreement with the previous studies [*Rau et al*., 1987; *Junium and Arthur*, 2007] that suggest high water-column denitrification during OAE2 based on nitrogen isotope records. In contrast, *Algeo et al*. [2014] suggest, based on model results for the global ocean and long-term N isotopic records of the Phanerozoic, that during OAEs the contribution of sedimentary denitrification was higher than that of the water column. However, their results do not exclude high water-column denitrification in semirestricted marine basins such as the proto-North Atlantic.

Our model results show a strong spatial heterogeneity (Figure 5b), where the central open ocean (W1) acts as both a major sink and source for N. Denitrification and N_2-fixation in the central open ocean (W1) represent about 44% of the total N outputs and 20% of the total N inputs in the basin, with rates as high as 11 and 5.2 Tmol yr^{-1}, respectively.

Our model suggests high rates of denitrification in both the central (W1) and the southern (W2) open ocean. Coastal denitrification, however, is more important in the Western Interior (W3) than in the euxinic southern proto-North Atlantic (W2 and W5), contrary to what is commonly assumed based on mainly southern observations [e.g., *Jenkyns et al*., 2007; *Junium and Arthur*, 2007]. In contrast, N inputs from N_2 fixers are important throughout the entire proto-North Atlantic, especially where primary productivity is high. This suggests that N_2-fixation was a major process that helped maintain elevated primary productivity rates, in good agreement with recent interpretations of geological records during OAE2 [*Ohkouchi et al*., 2006; *Blumenberg and Wiese*, 2012; *Zhang et al*., 2014]. In the BsLi-N run, the southern open ocean (W2) fixes about 2.8 Tmol N yr^{-1} during OAE2, which is only about 16% of the total N_2-fixation in the basin. Our results suggest that N_2-

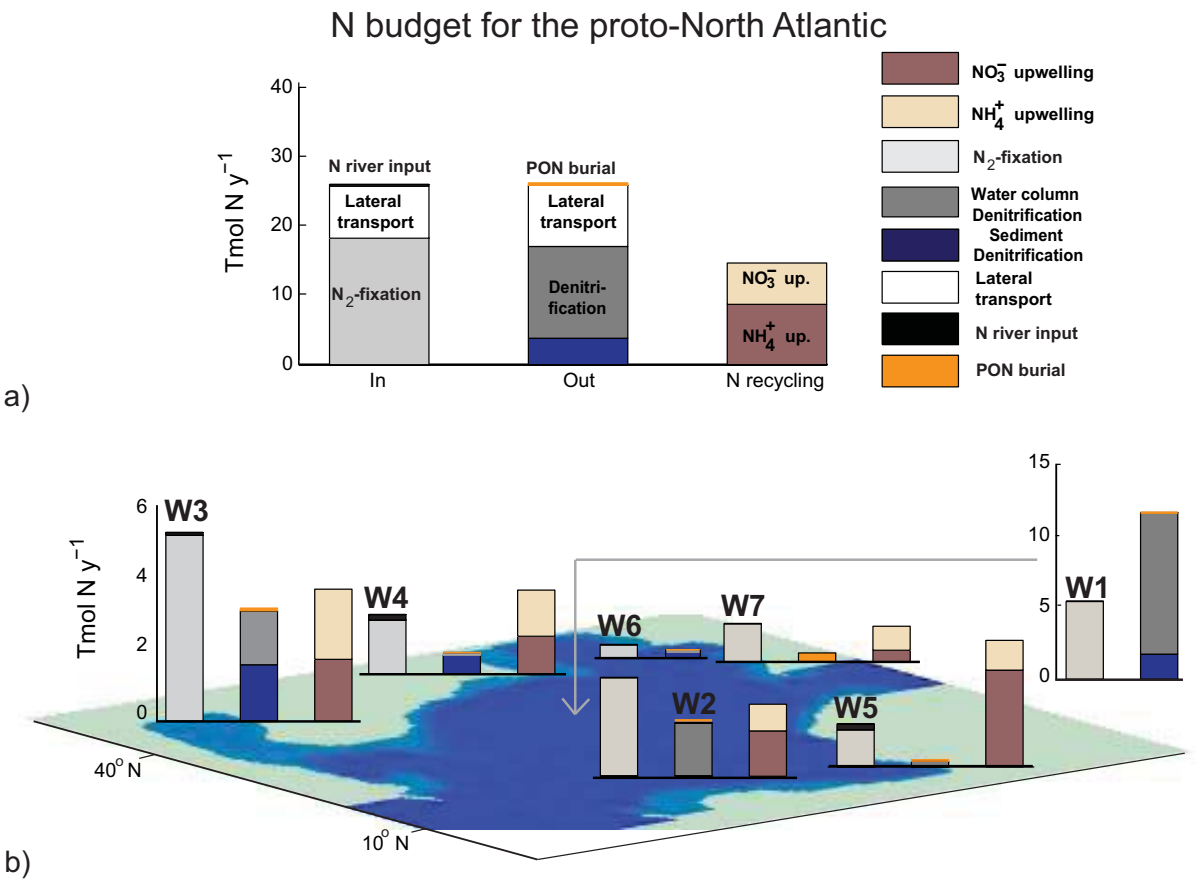

Figure 5. Steady state N budget for the proto-North Atlantic as estimated for OAE2 in the BsLi-N run; (a) total N sources and sinks for the proto-North Atlantic. Recycling N fluxes from remineralization of organic matter are indicated as either NO_x^- or NH_4^+; (b) regional contribution of the sources, sinks, and recycling of N. The regional lateral transport of N is not included in Figure 5b since it does not affect the proto-North Atlantic budget. The *y* axis in the open ocean (W1) is added because it is the only region where rates are larger than 10 Tmol yr^{-1} (i.e., in all other regions, the *y* axis ranges from 0 to 6, as indicated for the Western Interior, W3).

fixation in the Western Interior (W2) and in the central open ocean (W1) may have been of equal importance to the global N budget.

In the BsLi-N run, both total NH_4^+ upwelling and lateral N transport are about half the magnitude of N_2-fixation in the proto-North Atlantic (Figure 5a). Upwelling of NH_4^+ contributes to phytoplankton growth, as suggested by *Higgins et al*. [2012], but is not the ultimate source of N in the proto-North Atlantic. The role of recycled NH_4^+ varies spatially due to regional differences in upwelling/downwelling and organic matter degradation.

5. Conclusions

Our biogeochemical model for the proto-North Atlantic, that includes the N cycle, captures spatial trends in oxygen concentrations and POC burial as deduced from sediment records. Our model results confirm the hypothesis that enhanced availability of P could have fueled N_2-fixation and, therefore, primary productivity during OAE2. This implies that N_2-fixation compensated for the losses of N through denitrification and, by acting as a major N source, contributed to the severe oxygen depletion in the proto-North Atlantic. However, our model shows a spatial decoupling of N_2-fixation and denitrification. While N_2-fixation was widespread in surface waters, denitrification occurred mainly in the water column of the central basin and to a lesser extent along the coast. This spatial variability highlights that biogeochemical processes counteracted the homogeneous distribution of nutrients resulting from strong lateral and vertical transports. The N cycle slightly dampened the positive phosphorus-anoxia feedback loop during OAE2 conditions. Because of this interplay of the N and P cycles, both a P limited and a N-P colimited ocean behave similarly during OAE2.

Our model suggests that the volume of anoxic waters in the mid-Cretaceous global ocean at least doubled during OAE2. Due to this oxygen depletion, the predominant form of available inorganic N was likely ammonium instead of nitrate and, therefore, recycling of NH_4^+ became important for phytoplankton growth in all upwelling regions.

Acknowledgments
Special thanks to Dr. Dan Reed who helped improve the model efficiency. This research was funded by a "Focus & Massa project" granted to C.P. Slomp and H. Brinkhuis by the Utrecht University and by the European Research Council under the European Community's Seventh Framework Program, ERC Starting grant 278364. Additional financial support was provided by Statoil and the Netherlands Earth System Science Center. The code of the model can be requested by sending an email to the first author of this paper.

References

Algeo, T. J., P. A. Meyers, R. S. Robinson, H. Rowe, and G. Q. Jiang (2014), Icehouse-greenhouse variations in marine denitrification, *Biogeosciences*, *11*, 1273–1295.

Andersson, J. H., C. Woulds, M. Schwartz, G. L. Cowie, L. A. Levin, K. Soetaert, and J. J. Middelburg (2008), Short-term fate of phyto detritus in sediments across the Arabian Sea Oxygen Minimum Zone, *Biogeosciences*, *5*, 43–53.

Bertics, V. J., C. R. Löscher, I. Salonen, A. W. Dale, R. A. Schmitz, and T. Treude (2013), Occurrence of benthic microbial nitrogen fixation coupled to sulfate reduction in the seasonally hypoxic Eckernförde Bay, Baltic Sea, *Biogeosciences*, *10*, 1243–1258.

Blättler, C. L., H. C. Jenkyns, L. M. Reynard, and G. M. Henderson (2011), Significant increases in global weathering during Oceanic Anoxic Events 1a and 2 indicated by calcium isotopes, *Earth Planet. Sci. Lett.*, *309*(1–2), 77–88.

Blumenberg, M., and F. Wiese (2012), Imbalanced nutrients as triggers for black shale formation in a shallow shelf setting during the OAE 2 (Wunstorf, Germany), *Biogeosciences*, *9*, 4139–4153.

Breitbarth, E., A. Oschlies, and J. LaRoche (2007), Physiological constraints on the global distribution of Trichodesmium: Effect of temperature on diazotrophy, *Biogeosciences*, *4*(1), 53–61.

Capone, D. G., and E. J. Carpenter (1982), Nitrogen fixation in the marine environment, *Science*, *217*(4565), 1140–1142.

Carr, N. G., and B. A. Whitton (1982), *The Biology of Cyanobacteria*, vol. 19, Univ. of Calif. Press, Calif.

Codispoti, L. A. (2007), An oceanic fixed nitrogen sink exceeding 400 Tg N a^{-1} vs the concept of homeostasis in the fixed-nitrogen inventory, *Biogeosciences*, *4*(2), 233–253.

Codispoti, L. A., T. Yoshinari, and A. H. Devol (2005), Suboxic respiration in the oceanic water column, in *Respiration in Aquatic Ecosystems*, edited by P. A. del Giorgio and P.J. le B. Williams, pp. 225–247, Oxford Univ. Press, N. Y.

DeVries, T., C. Deutsch, P. A. Rafter, and F. Primeau (2013), Marine denitrification rates determined from a global 3-D inverse model, *Biogeosciences*, *10*(4), 2481–2496.

Dyhrman, S. T., J. W. Ammerman, and B. A. S. Van Mooy (2007), Microbes and the marine phosphorus cycle, *Oceanography*, *20*(2), 110–116.

Falcón, L. I., E. J. Carpenter, F. Cipriano, B. Bergman, and D. G. Capone (2004), N_2 fixation by unicellular bacterioplankton from the Atlantic and Pacific Oceans: Phylogeny and in situ rates, *Appl. Environ. Microbiol.*, *70*(2), 765–770.

Falkowski, P. G. (1997), Evolution of the nitrogen cycle and its influence on the biological sequestration of CO_2 in the ocean, *Nature*, *387*(6630), 272–275.

Fashman, M. J. R. (2003), *Ocean Biogeochemistry: The Role of the Ocean Carbon Cycle in Global Change*, Springer, Berlin.

Fernandez, C., L. Farías, and O. Ulloa (2011), Nitrogen fixation in denitrified marine waters, *PLoS One*, *6*(6), 1–9.

Flögel, S., K. Wallmann, C. J. Poulsen, J. Zhou, A. Oschlies, S. Voigt, and W. Kuhnt (2011), Simulating the biogeochemical effects of volcanic CO_2 degassing on the oxygen-state of the deep ocean during the Cenomanian-Turonian Anoxic Event (OAE2), *Earth Planet. Sci. Lett.*, *305*, 371–384.

Fulweiler, R. W., S. W. Nixon, B. A. Buckley, and S. L. Granger (2008), Net sediment N_2 fluxes in a coastal marine system—Experimental manipulations and a conceptual model, *Ecosystems*, *11*(7), 1168–1180.

Galloway, J. N., et al. (2004), Nitrogen cycles: Past, present, and future, *Biogeochemistry*, *70*(2), 153–226.

Gruber, N. (2004), The dynamics of the marine nitrogen cycle and its influence on atmospheric CO_2 variations, in *The Ocean Carbon Cycle and Climate*, pp. 97–148, Springer, Netherlands.

Gruber, N., and J. N. Galloway (2008), An Earth-system perspective of the global nitrogen cycle, *Nature*, *451*(7176), 293–296.

Handoh, I. C., and T. M. Lenton (2003), Periodic mid-Cretaceous oceanic anoxic events linked by oscillations of the phosphorus and oxygen biogeochemical cycles, *Global Biogeochem. Cycles*, *17*(4), 1092, doi:10.1029/2003GB002039.

Higgins, M. B., R. S. Robinson, J. M. Husson, S. J. Carter, and A. Pearson (2012), Dominant eukaryotic export production during ocean anoxic events reflects the importance of recycled NH_4^+, *Proc. Natl. Acad. Sci. U. S. A.*, *109*(7), 2269–2274.

Houghton, R. A. (2007), Balancing the global carbon budget, *Annu. Rev. Earth Planet. Sci.*, *35*, 313–347.

Howarth, R. W., R. Marino, and J. J. Cole (1988), Nitrogen fixation in freshwater, estuarine, and marine ecosystems. 2. Biogeochemical controls, *Limnol. Oceanogr.*, *33*(4), 688–701.

Hutchins, D. A., F.-X. Fu, Y. Zhang, M. E. Warner, Y. Feng, K. Portune, P. W. Bernhardt, and M. R. Mulholland (2007), CO_2 control of Trichodesmium N_2 fixation, photosynthesis, growth rates, and elemental ratios: Implications for past, present, and future ocean biogeochemistry, *Limnol. Oceanogr. Methods*, *52*(4), 1293–1304.

Jenkyns, H. C. (2010), Geochemistry of oceanic anoxic events, *Geochem. Geophys. Geosyst.*, *11*, Q03004, doi:10.1029/2009GC002788.

Jenkyns, H. C., A. Matthews, H. Tsikos, and Y. Erel (2007), Nitrate reduction, sulfate reduction, and sedimentary iron isotope evolution during the cenomanian-turonian oceanic anoxic event, *Paleoceanography*, *22*, PA3208, doi:10.1029/2006PA001355.

Junium, C. K., and M. A. Arthur (2007), Nitrogen cycling during the Cretaceous, Cenomanian-Turonian Oceanic Anoxic Event II, *Geochem. Geophys. Geosyst.*, *8*, Q03002, doi:10.1029/2006GC001328.

Kantartzi, S., E. Vaiopoulou, A. Kapagiannidis, and A. Aivasidis (2006), Kinetic characterization of nitrifying pure cultures in chemostate, *Global NEST*, *2*(2), 2.

Karl, D., et al. (2002), *Dinitrogen Fixation in the World's Oceans*, pp. 47–98, Springer, Netherlands.

Knapp, A. N., J. Dekaezemacker, S. Bonnet, J. A. Sohm, and D. G. Capone (2012), Sensitivity of *Trichodesmium erythraeum* and *Crocosphaera watsonii* abundance and N2 fixation rates to varying NO_3^- and PO_4^{3-} concentrations in batch cultures, *Aquat. Microb. Ecol.*, *66*, 223–236.

Konovalov, S. K., L. I. Ivanov, and A. S. Samodurov (2000), Oxygen, nitrogen and sulphide fluxes in the Black Sea, *Mediter. Mar. Sci.*, *1*(2), 41–59.

Konovalov, S. K., C. A. Fuchsman, V. Belokopitov, and J. W. Murray (2008), Modeling the distribution of nitrogen species and isotopes in the water column of the Black Sea, *Mar. Chem.*, *111*(12), 106–124.

Kraal, P., C. P. Slomp, A. Forster, and M. M. M. Kuypers (2010b), Phosphorus cycling from the margin to abyssal depths in the proto-Atlantic during oceanic anoxic event 2, *Palaeogeogr. Palaeoclimatol. Palaeoecol.*, *295*, 42–54.

Kuypers, M. M. M., R. D. Pancost, I. A. Nijenhuis, and J. S. Sinninghe Damsté (2002), Enhanced productivity led to increased organic carbon burial in the euxinic North Atlantic basin during the late Cenomanian oceanic anoxic event, *Paleoceanography*, *17*(4), 1051, doi:10.1029/2000PA000569.

Kuypers, M. M., Y. van Breugel, S. Schouten, E. Erba, and J. S. Sinninghe Damsté (2004a), N_2-fixing cyanobacteria supplied nutrient N for Cretaceous oceanic anoxic events, *Geology*, *32*(10), 853–856.

Kuypers, M. M. M., L. J. Lourens, W. I. C. Rijpstra, R. D. Pancost, I. A. Nijenhuis, and J. S. Sinninghe Damsté (2014b), Orbital forcing of organic carbon burial in the proto-North Atlantic during oceanic anoxic event 2, *Earth Planet. Sci. Lett.*, *228*(4), 465–482.

Lam, P., and M. M. Kuypers (2011), Microbial nitrogen cycling processes in oxygen minimum zones, *Annu. Rev. Mar. Sci.*, *3*(1), 317–345.

Lam, P., G. Lavik, M. M. Jensen, J. van de Vossenberg, M. Schmid, and D. Woebken (2009), Revising the nitrogen cycle in the peruvian oxygen minimum zone, *Proc. Natl. Acad. Sci. U. S. A.*, *106*(12), 4752–4757.

Lenton, T. M., and A. J. Watson (2000), Redfield revisited: 1. Regulation of nitrate, phosphate, and oxygen in the ocean, *Global Biogeochem. Cycles*, *14*(1), 225–248.

Longhurst, A., S. Sathyendranath, T. Platt, and C. Caverhill (1995), An estimate of global primary production in the ocean from satellite radiometer data, *J. Plankton Res.*, *17*(6), 1245–1271.

Middelburg, J. J., and L. A. Levin (2009), Coastal hypoxia and sediment biogeochemistry, *Biogeosciences*, *6*, 1273–1293.

Middelburg, J. J., K. Soetaert, P. M. J. Herman, and C. H. R. Heip (1996), Denitrification in marine sediments: A model study, *Global Biogeochem. Cycles*, *10*(4), 661–673.

Millero, F. J. (1996), *Chemical Oceanography*, 2nd ed., CRC Press, Boca Raton.

Mills, M. M., C. Ridame, M. Davey, J. La Roche, and R. J. Geider (2004), Iron and phosphorus co-limit nitrogen fixation in the eastern tropical North Atlantic, *Nature*, *429*(6989), 292–294.

Moffett, J. W., T. J. Goepfert, and S. Naqvi (2007), Reduced iron associated with secondary nitrite maxima in the Arabian Sea, *Deep Sea Res., Part I*, *54*(8), 1341–1349.

Monteiro, F. M., R. D. Pancost, A. Ridgwell, and Y. Donnadieu (2012), Nutrients as the dominant control on the spread of anoxia and euxinia across the Cenomanian–Turonian oceanic anoxic event (OAE2): Model-data comparison, *Paleoceanography*, *27*, PA4209, doi:10.1029/2012PA002351.

Moore, C. M., et al. (2013), Processes and patterns of oceanic nutrient limitation, *Nat. Geosci.*, *6*(9), 701–710.

Mort, H. P., T. Adatte, K. B. Föllmi, G. Keller, P. Steinmann, V. Matera, Z. Berner, and D. Stüben (2007), Phosphorus and the roles of productivity and nutrient recycling during oceanic anoxic event 2, *Geology*, *35*, 483–486.

Murray, J. W., et al. (1995), Oxidation-reduction environments: The suboxic zone in the Black Sea, *ACS Adv. Chem. Ser.*, *244*, 157–176.

Naqvi, S. W. A., H. Naik, A. Pratihary, W. D'Souza, P. V. Narvekar, D. A. Jayakumar, A. H. Devol, T. Yoshinari, and T. Saino (2006), Coastal versus open-ocean denitrification in the Arabian Sea, *Biogeosciences*, *3*(4), 621–633.

Nederbragt, A. J., J. Thurow, H. Vonhof, and H.-J. Brumsack (2004), Modelling oceanic carbon and phosphorus fluxes: Implications for the cause of the late Cenomanian Oceanic Anoxic Event (OAE2), *J. Geol. Soc. London*, *161*(4), 721–728.

Ohkouchi, N., Y. Kashiyama, J. Kuroda, N. O. Ogawa, and H. Kitazato (2006), The importance of diazotrophic cyanobacteria as primary producers during Cretaceous Oceanic Anoxic Event 2, *Biogeosciences*, *3*(4), 467–478.

Omstedt, A., E. Gustafsson, and K. Wesslander (2009), Modelling the uptake and release of carbon dioxide in the Baltic Sea surface water, *Cont. Shelf Res.*, *29*(7), 870–885.

Owens, J. D., T. W. Lyons, X. Li, K. G. Macleod, G. Gordon, M. M. M. Kuypers, A. Anbar, W. Kuhnt, and S. Severmann (2012), Iron isotope and trace metal records of iron cycling in the proto-North Atlantic during the Cenomanian-Turonian oceanic anoxic event (OAE-2), *Palaeogeography*, *27*, PA3223, doi:10.1029/2012PA002328.

Ozaki, K., S. Tajima, and E. Tajika (2011), Conditions required for oceanic anoxia/euxinia: Constraints from a one-dimensional ocean biogeochemical cycle model, *Earth Planet. Sci. Lett.*, *304*(1), 270–279.

Paulmier, A., and D. Ruiz-Pino (2009), Oxygen minimum zones (OMZs) in the modern ocean, *Prog. Oceanogr.*, *80*(3), 113–128.

Planavsky, N. J., O. J. Rouxel, A. Bekker, S. V. Lalonde, K. O. Konhauser, C. T. Reinhard, and T. W. Lyons (2010), The evolution of the marine phosphate reservoir, *Nature*, *467*, 1088–1090.

Quan, T. M., and P. G. Falkowski (2009), Redox control of N:P ratios in aquatic ecosystems, *Geobiology*, *7*(2), 124–139.

Rabouille, C., F. T. Mackenzie, and L. May Ver (2001), Influence of the human perturbation on carbon, nitrogen, and oxygen biogeochemical cycles in the global coastal ocean, *Geochim. Cosmochim. Acta*, *65*(21), 3615–3641.

Rau, G. H., M. A. Arthur, and W. E. Dean (1987), $^{15}N/^{14}N$ variations in Cretaceous Atlantic sedimentary sequences: Implication for past changes in marine nitrogen biogeochemistry, *Earth Planet. Sci. Lett.*, *82*(3), 269–279.

Risgaard-Petersen, N., R. L. Meyer, and N. P. Revsbech (1993), Denitrification and anaerobic ammonium oxidation in sediments: Effects of microphytobenthos and NO_3^-, *Aquat. Microb. Ecol.*, *107*, 405–409.

Ruvalcaba Baroni, I., R. P. M. Topper, N. A. G. M. van Helmond, H. Brinkhuis, and C. P. Slomp (2014), Biogeochemistry of the North Atlantic during oceanic anoxic event 2: Role of changes in ocean circulation and phosphorus input, *Biogeosciences*, *11*(4), 977–993.

Sañudo-Wilhelmy, S. A., A. B. Kustka, C. J. Gobler, D. A. Hutchins, M. Yang, K. Lwiza, J. Burns, D. G. Capone, J. A. Raven, and E. J. Carpenter (2001), Phosphorus limitation of nitrogen fixation by *Trichodesmium* in the central Atlantic Ocean, *Nature*, *411*(6833), 66–69.

Schlanger, S. O., and H. C. Jenkyns (1976), Cretaceous oceanic anoxic events: Causes and consequences, *Geol. Mijnbouw*, *55*(3–4), 179–184.

Sinninghe Damsté, J. S., and J. Köster (1998), A euxinic southern North Atlantic Ocean during the Cenomanian-Turonian oceanic anoxic event, *Earth Planet. Sci. Lett.*, *158*, 165–173.

Sinninghe Damsté, J. S., E. C. van Bentum, G.-J. Reichart, P. Pross, and S. Schouten (2010), A CO_2 decrease-driven cooling and increased latitudinal temperature gradient during the mid-Cretaceous Oceanic Anoxic Event 2, *Earth Planet. Sci. Lett.*, *293*(1–2), 97–103.

Slomp, C. P., and P. Van Cappellen (2007), The global marine phosphorus cycle: Sensitivity to oceanic circulation, *Biogeosciences*, *4*, 155–171.

Staal, M., F. J. R. Meysman, and L. J. Stal (2003), Temperature excludes N_2-fixing heterocystous cyanobacteria in the tropical oceans, *Nature*, *425*(6957), 504–507.

Topper, R. P. M., J. Trabucho Alexandre, E. Tuenter, and P. Th. Meijer (2011), A regional ocean circulation model for the mid-Cretaceous North Atlantic Basin: Implications for black shale formation, *Clim. Past*, *7*, 277–297.

Trabucho Alexandre, J., E. Tuenter, G. A. Henstra, R. S. W. van der Zwan, K. J. van de Wal, H. A. Dijkstra, and P. L. de Boer (2010), The mid-Cretaceous North Atlantic nutrient trap: Black shales and OAEs, *Paleoceanography*, *25*, PA4201, doi:10.1029/2010PA001925.

Tsandev, I., and C. P. Slomp, Modeling phosphorus cycling and carbon burial during Cretaceous Oceanic Anoxic Events (2009), *Earth Planet. Sci. Lett.*, *286*(1), 71–79.

Tyrrell, T. (1999), The relative influences of nitrogen and phosphorus on oceanic primary production, *Nature*, *400*, 525–531.

van Bentum, E. C., G.-J. Reichart, and J. S. Sinninghe-Damsté (2012), Organic matter provenance, palaeoproductivity and bottom water anoxia during the Cenomanian/Turonian oceanic anoxic event in the Newfoundland Basin (northern proto North Atlantic Ocean), *Org. Geochem.*, *50*, 11–18.

Vermeij, G. J. (1995), Economics, volcanoes, and Phanerozoic revolutions, *Paleobiology*, *21*(2), 125–152.

Voigt, S. (2000), Cenomanian-Turonian composite $\delta^{13}C$ curve for Western and Central Europe: The role of organic and inorganic carbon fluxes, *Palaeogeogr. Palaeoclimatol. Palaeoecol.*, *160*, 91–104.

Wallmann, K. (2003), Feedbacks between oceanic redox states and marine productivity: A model perspective focused on benthic phosphorus cycling, *Global Biogeochem. Cycles*, *17*(3), 1084, doi:10.1029/2002GB001968.

Wasmund, N., M. Voss, and K. Lochte, (2001), Evidence of nitrogen fixation by non-heterocystous cyanobacteria in the Baltic Sea and re-calculation of a budget of nitrogen fixation, *Mar. Ecol. Prog. Ser.*, *214*(1988), 1–14.

Weber, T., and C. Deutsch (2012), Oceanic nitrogen reservoir regulated by plankton diversity and ocean circulation, *Nature*, *489*(7416), 419–422.

Weber, T. S., and C. Deutsch (2010), Ocean nutrient ratios governed by plankton biogeography, *Nature*, *467*(7315), 550–554.

Zerkle, A. L., C. H. House, R. P. Cox, and D. E. Canfield (2006), Metal limitation of cyanobacterial N_2 fixation and implications for the Precambrian nitrogen cycle, *Geobiology*, *4*(4), 285–297.

Zhang, X., D. M. Sigman, F. M. M. Morel, and A. M. L. Kraepiel (2014), Nitrogen isotope fractionation by alternative nitrogenases and past ocean anoxia, *Proc. Natl. Acad. Sci. U. S. A.*, *111*(13), 4782–4787.